

A Uhf Near Field RFID Reader Antenna Implemented with Fractal Koch Curve

ChitraVaradhan^a and DrArulselvi^b

^a Research Scholar Department of ECE, Bharath Institute of Higher Education and Research, Chennai, Tamilnadu, India - 600 073

^b Associate Professor, Department of ECE, Bharath Institute of Higher Education and Research, Chennai, Tamilnadu, India - 600 073

Article History: Received: 10 January 2021; Revised: 12 February 2021; Accepted: 27 March 2021; Published online: 28 April 2021

Abstract: This paper comprises a fractal Koch curve with tapered slot structure subjected to magnetic field strength analysis for Ultra High Frequencies (UHF) RFID near field reader antenna. In the design, Variable distance with opposite direction current principle is used. The center frequency of the proposed antenna operates at 897 MHz with bandwidth of 101 MHz (853 to 954 MHz). The obtained bandwidth is sufficient to cover the UHF RFID frequency for, Canada (902-928 MHz), Europe and USA (865-868 MHz). The near field analysis was verified by keeping different liquids and the antenna performance is calculated. During the measurement, the antenna is kept at a distance of 50 mm in z direction and is observed that the interrogation area of proposed antenna is achieved with 243 mm X 190 mm. The result shows that the antenna exhibits the ability to track chemicals in industries and pharmaceutical applications management. It is also observed that the proposed antenna is sufficient to operate as commercial tags for near field magnetic induction communication.

Key words—Fractal Koch curve, near field magnetic induction communication, UHF RFIDs, opposite direction current

I. Introduction

The self-similar configuration is observed from nature, which are referred as fractal geometries. For example, the shape of the cloud, leaf structures may represent the fractal geometries. These geometries introduced in the year 1975, each sub-section has similar small scale characteristics to the whole entity. Fractal geometries have self-similarity property which have been effectively utilised in various engineering technologies like in the design antennas and radiators. In general, fractal structures lead to reduction of the physical size of antenna and it produces multiband behaviour in radiation characteristics. Also, the design has the capability to exhibit long path in small volume. The shape of radiating element can be configured by iterative mathematical process to achieve multiband behaviour and self-similarity property used for antenna miniaturization. [1&2].

Radio Frequency Identification (RFID) is an emerging technology, in which RF signals are used to identify the objects automatically. A few applications are employee attendance, library book management, goods management in industries and toll fee collections. RFID consists of two important elements Reader and tag. The major challenge in RFID tag performance is mainly affected by the electrical properties of objects surrounding the tag, due to which the antenna impedance may be affected. Metals and liquids are common materials affecting the performance of antenna.

According to the application specifications the mobility of the tag is divided into high, medium and low mobility of tags. SHF RFIDs are used for high mobility applications. When the frequency is high, the time taken for the signal to travel is very short. Therefore, fast object tracking is achieved. But the signal degradation occurs due to the presence of liquid and metals. In goods management applications, the mobility of the tag is not entertained much, but there is a signal distortion due to the obstruction. The UHF RFIDs (generally 900 MHz) are near field RFIDs (NF RFIDs), in that the magnetic field coupling of RF power takes place. The key features such as smaller tag, reading stability and maximum power transfer makes UHF near field RFIDs a front end in many applications such as item level tagging and smart shelves [3&4].

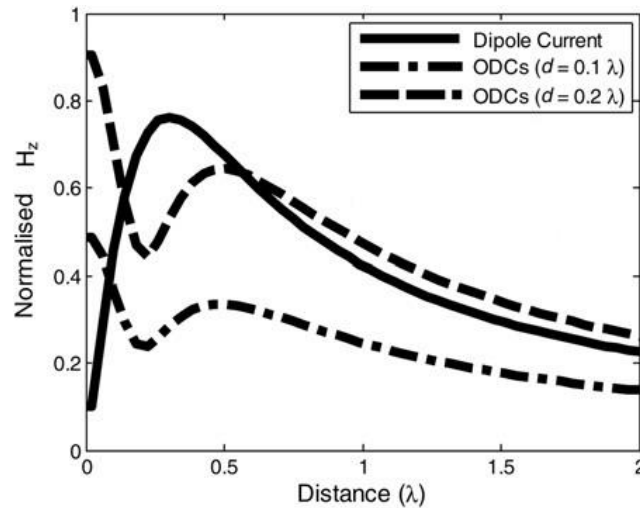


Figure. 1. Magnetic field as a function of distance between ODC elements

Tracking of chemical in pharmaceutical industries are facing issues due to the presence of hindrances in the near field region. The RFID tags fixed on the containers containing liquids like acids and drugs, causes communication obstruction in between reader and tag.

The next challenge is the antenna size. The magnetic field intensity is increased by large electrical structure of radiating part, which increases the size of the antenna. [5]. To generate a strong HZ in the near field region of the antenna, loop structures can be used. But the loop or segmented loop fails to generate uniform magnetic field. The opposite direction current (ODC) principle can be incorporated to achieve strong uniform magnetic field near the antenna.

The European UHF RFID range is 865-868 MHz whereas USA and Canada uses 902-928 MHz for UHF RFIDs. So the third factor considered is bandwidth. Acquiring a wide band should be adequate for both the range of RFID applications.

Considering all the above problems, the communication proposed is a UHF RFID reader antenna for near field application with 90 mm X 90 mm size. The center frequency falls on both European and USA UHF ranges. The near field analysis shows that the proposed antenna maintains adequate field strength even with the fluid obstructions present in chemical industries.

The magnetic field generation is explained in the II section, while section III describes the design of proposed antenna. This section IV discusses the simulated results and related details, while prototype fabrication and measured results are presented in section V.

Generation of Magnetic Field

A. Principle of Opposite Direction Current

From the surveys, an intense magnetic field can be obtained by the opposite direction current principle. The adjacent dipoles generate reinforcement of magnetic field in intended region and the current flows with 180° out of phase. But implementing dual feed techniques increases the design complexity. Hence single feed with ODC principle is used in the proposed antenna. [6]

Earlier researchers proposed the tapered slot structures for high frequency and high directivity applications. The principle is applied at the tapered slot opening boundaries. [7]. In this paper, the distance between the dipole pair is increased gradually to generate a strong magnetic field in near field.

B. Importance of Fractal Structure

The Koch fractal curve is implemented in the TSA, hence reducing the antenna size without compromising the frequency of operation. [8]. Second iteration of fractal Koch curve is used to bring the size of antenna to 90 mm x 90 mm. The fractal flanges helps to pass the current through 0.3λ gap between the pair of dipoles and this space is adequate to generate a strong and uniform magnetic field.

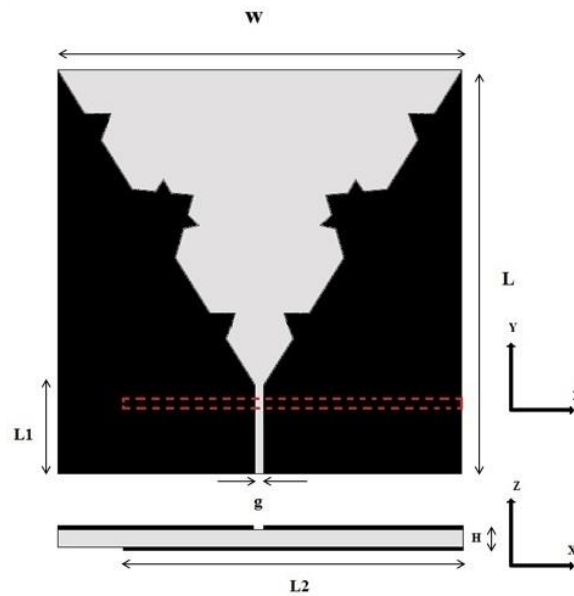


Figure 2:Proposed antenna diagram

Design of Antenna

The suggested antenna consists of V shape fractal slot opening and a Microstrip line used to excite the antenna from the rear. This is exhibited in the figure 2 in hyphenated red lines.

A. Design of Microstrip Line

The dimensions of line width, patch height (35 μm) and the patch are deposited on the substrate, as per the industry standard. Impedance 50-ohm microstrip line is estimated by the equation (1). Table 1 describes the proposed antenna dimensions.

$$Z_0 = \frac{60}{\sqrt{\epsilon_r}} \ln \left(\dots \dots \dots \right) \quad (1)$$

Table 1: Antenna Dimension

Label	Quantity
W	90 mm
L	90mm
L1	18mm
L2	7m
H	1.6 mm
g	2 mm

B. Design of Fractal Protrusion

Fractals have two important properties such as self-similarity and space filling patterns. These properties help to get effective radiation in the near field. Koch curve is introduced in the antenna design to achieve strong HZ as well as miniaturization of antenna. Fractal structure helpin creation of three field generating zones and diagonal edges of dipole pair configured in the proposed design. Feed point slot width is kept as 2 mm which is meagre compared to wavelength, hence production of magnetic field is very less initially. The flared profile is introduced to increase the distance between the ODC pair spacing, results in sufficient increase of magnetic field. Figure 3 shows the spacing between the edges as 0.03λ,0.1λ,0.2λ which generates strong magnetic field in the near field.

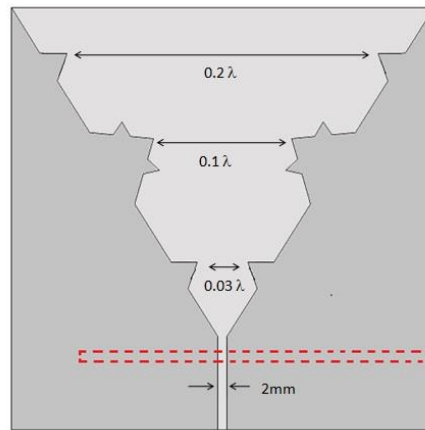


Figure.3. Distance Between the Dipoles. A gradual increase from 2mm to 0.2λ .

Simulation Result and Analysis

Surface Current Distribution

Surface current distribution analysis is very important in near field analysis. The phase angle of surface current distribution is corresponding to 0 and 90 degrees. The surface current distribution over the plane is shown in figure 4 (A & B). From the Figure 4, it is verified that, the opposite current is uniformly distributed over the antenna surface.

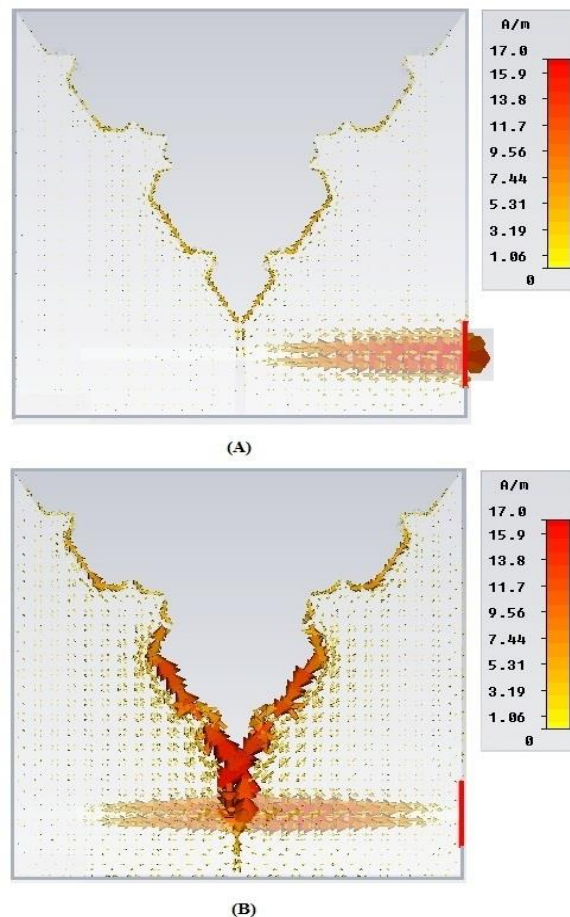


Figure 4: Surface Current Distribution at 0 (Figure 4 A) and 90 (Figure 4 B) Degree Respectively

S₁₁ Characteristics

The S_{11} parameter shows the frequency span starts with 400 MHz to 1.41 GHz, which is depicted in Figure 5. From the figure it can be concluded that the suggested antenna operates at 897MHz. At -10dB the measured impedance bandwidth is 102 MHz and the obtained simulated bandwidth is 130 MHz and at center frequency the value of S_{11} is -29.5dB, which is nominal compared to other literature surveys. The measured results are highly

correlated with simulation results. The measured band width is sufficient to operate for UHF- RFID at Europe, USA and Canada. The amount of signal and noise entering in to the antenna will be less because the measured band width is sufficient to cover the requirement of above mentioned countries bands. Hence the proposed antenna offers excellent noise immunity.

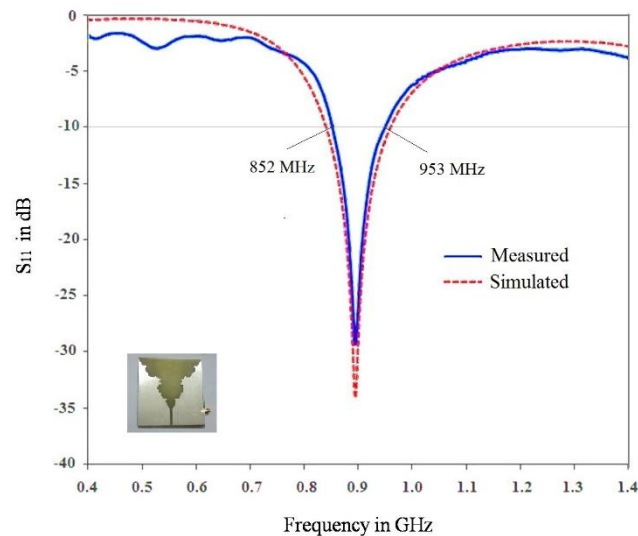


Figure 5: S_{11} vs. Frequency Graph for the Antenna. The Simulated & Measured Results

VSWR Bandwidth

Voltage Standing Wave Ratio is another important parameter in antenna design engineering. To determine the bandwidth, VSWR was measured with 2 as the reference line. From the figure 8, it is apparent that the proposed antenna gives VSWR bandwidth of 133MHz within the range of 837 to 970 MHz. At the operating frequency, minimum Voltage Standing Wave Ratio of 1.03 is achieved around the frequency 897 MHz.

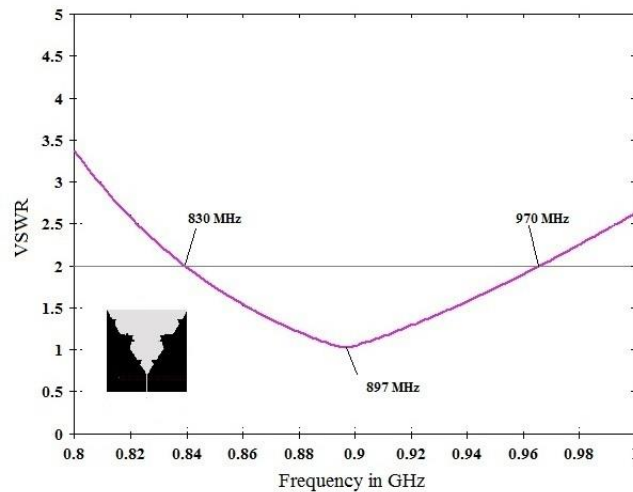


Figure. 6. The simulated result of VSWR vs. Frequency

Variable distance of Dipole Pair

To analyze the effects of changes in fractal geometry and ODC pair, the slot width distance is maintained as 0.2λ . The antenna generally produces strong magnetic field but when the ODC pair is fed, the slot line width changes the center frequency of proposed antenna. Tapered slot profile is introduced in the design and gradual increase of slot from 0.006λ to 0.3λ , results in the generation of a strong magnetic field. The fractal bends help to generate three field zones and slant edge opening in the structure of the antenna.

In near field analysis, the field generation is performed by the variable distance ODC principle. A strong magnetic field is generated with radial area of 190 mm x 240 mm is shown in figure 7(a) and it is experienced that there are no nulls present in the observation zone. The maximum magnetic field strength is -8.90 dB A/m at a distance of 50 mm. A cut in the xzplane at a height of 30 mm from the proposed antenna plane is shown in figure 7(b). A good amount of magnetic field distribution is observed in the near field region which is greater than -20dBA/m. This field distribution is sufficient to identify a commercial passive RFID tag. The simulated result provides ample read distance at 95mm from the antenna plane. Test tube with standard size are taken, filled

with oil, considering oil as an obstructive medium. The test tubes placed at distance of 35 mm from the antenna spaced with respect to each other at 2 mm. The simulated result shows that around 0.3dBA/m there is reduction in magnetic field, which is tolerable for chemical tracking. The simulated results is depicted in figure 7(c). As a part of the next trial phase, water was considered as obstruction. The glass test tubes filled with water are placed with same distance as in the previous trials. The result shows that a slight degradation 0.5 dBA/m was observed but quite readable. The corresponding simulated result is shown in figure 7(d).

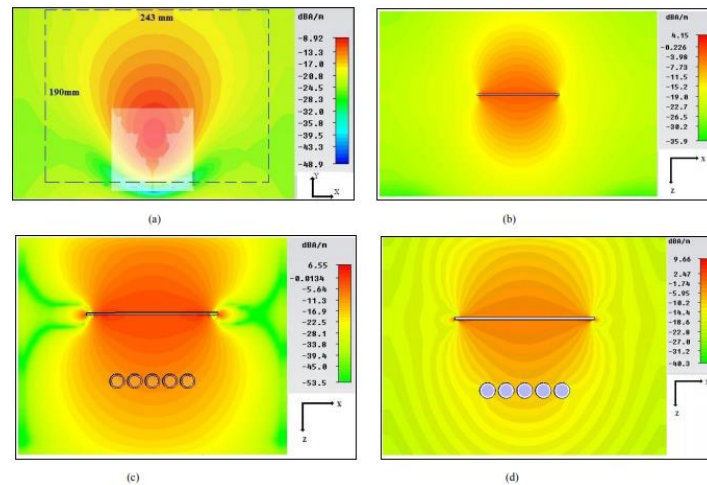


Figure 7: Magnetic Field Curves Observed from Center of Antenna (a) x-y plane at 50 mm at z direction. (b) x-z plane at 30mm. (c) x-z plane at 30 mm with oil container. (d) x-z plane at 30 mm with water container.

Fabrication of prototype and Measurement of results

Fabricated Antenna



Figure 8: Fabricated Prototype of Antenna

The designed antenna is fabricated on FR-4 substrate as shown in figure 8. FR-4 ($\epsilon_r= 4.4, \delta = 0.025$) material consists of adequate mechanical strength hence, a prototype was fabricated with a thickness of 1.6 mm. The micro-strip line is provided at the rear side of the antenna and deposited with perfect electric conductor (PEC). The thickness of the line is 0.035 mm. The same dimension is applied at the front panel of the antenna etched with fractal V shaped Koch protrusion. Low profile and simplicity is maintained because no active components were used in the fabrication of antenna. Minimal cost is achieved during the fabrication due to the accessibility of the material. SMA connector (50Ω impedance) was soldered with the micro-strip feed.

Measurement Setup and Near Field Measurement

The performance of the fabricated antenna was tested for measuring S_{11} parameter using Agilent E8363B vector network analyzer. The typical measurement arrangement of S_{11} parameter is shown in figure 9(a) while figure 9(b) shows the setup of near field measurement. The measurement helps to find the HZ. The measurement setup of the fabricated antenna is kept in semi-anechoic chamber. A microwave source with power of 13dBm is fed to the antenna. Foam fixture was assembled and the fabricated antenna was placed on it. A field meter is used to measure the performance of near field and the antenna was stimulated at 897 MHz. The obstructions were kept at a space of 5cm from the center of the antenna and magnetic field measurements were taken in the chamber without any compromise in the performance.

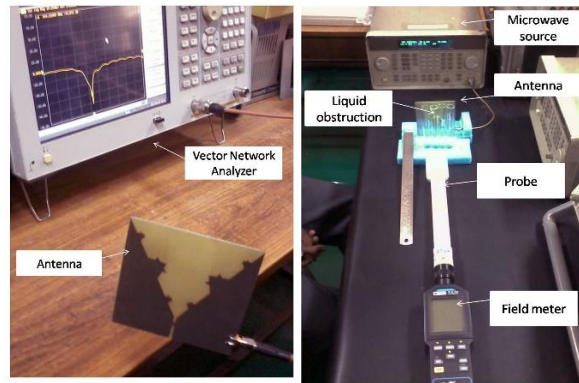


Figure 9. Measurement Arrangement with Fabricated Antenna.

Figure 9(a) The measurement of S_{11} parameter. Figure 9 (b) Indicates Nearfield measurement setup.

The Near field measurement observation from the center of the prototype of antenna is shown in figure 10. The read distance of 95 mm was found in the absence of obstruction. Considering oil as obstruction, small acceptable degradation was observed at 6 mm read distance and for water, the read distance is decreased by 8 mm, from the read distance in the absence of obstruction. Hence, it is proved in the communication that the read distance is reduced with respect to dielectric constant. The observed read distance and magnetic field strength is depicted as a graph in figure 11.

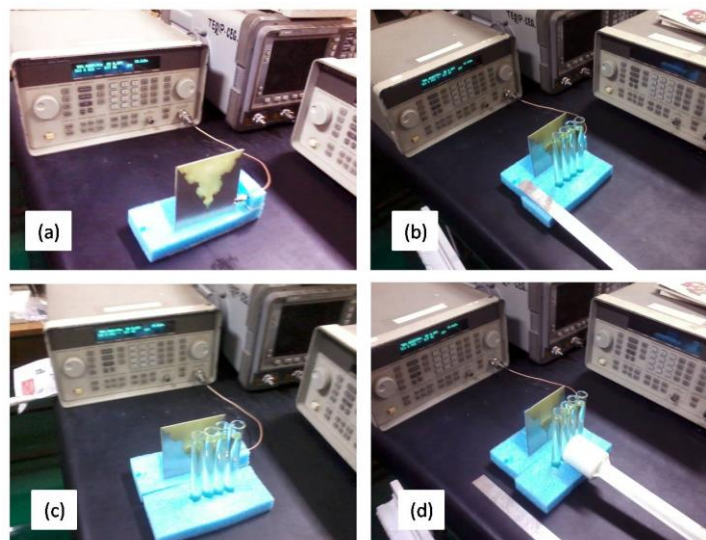


Figure 10. Measurement of Read Range in Near Field. (a) Fabricated Antenna without Obstruction. (b) Antenna with water as obstruction. (c) Antenna with oil as obstruction (d) Measurement of Hz.

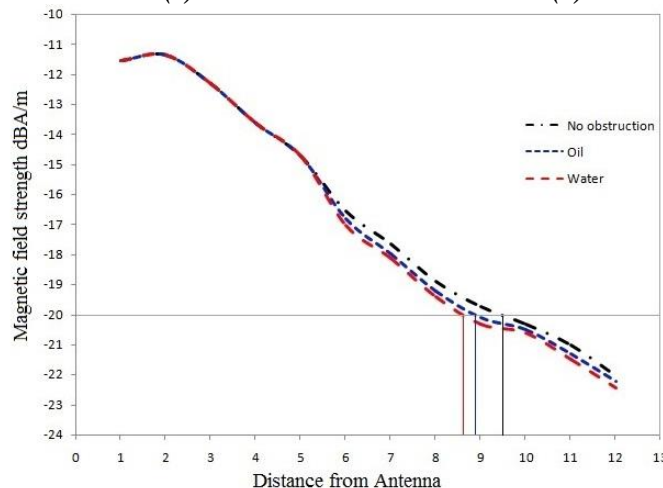


Figure 11. Magnetic field vs Distance from Antenna with and without obstruction

TABLE II Fabricated Prototype Antenna Parameters

S. No.	Antenna Parameter	Observed Result
1	Resonant frequency	897 MHz
2	Bandwidth Impedance	101 MHz (measured)
3	VSWR Band width	130 MHz (simulated)
4	S_{11} at resonant frequency	-29dB
5	Area of interrogation ($z= 50$ mm)	190mm x 243mm
6	Antenna size	90 mm x 90 mm
7	Antenna input power	13dBm
8	Read distance without obstruction	95 mm
9	Water as obstruction (Read distance)	87 mm
10	Oil as obstruction (Read distance)	89 mm

Conclusion

In this communication a RFID reader antenna is proposed with fractal Koch curve and a method is presented to generate uniform and strong magnetic field by implementing variable distance opposite distance current principle. The fabricated prototype antenna operated at 897 MHz, achieves a measurement of 101 MHz impedance bandwidth. The obtained bandwidth is sufficient to operate in European, USA and Canada UHF RFID bandwidth. The fabricated antenna provides excellent read range of 95 mm when there is no obstruction. The measurement of read range is extended by keeping water and oil as obstruction, resulting in satisfied performance for tracking the chemicals in industries and pharmaceutical management applications. The investigations can be extended to track the ornaments by testing the near field performance in the presence of metals.

References

1. J. B. Benavides, R. A. Lituma, P. A. Chasi and L. F. Guerrero, "A Novel Modified Hexagonal Shaped Fractal Antenna with Multi Band Notch Characteristics for UWB Applications," 2018 IEEE-APS Topical Conference on Antennas and Propagation in Wireless Communications (APWC), Cartagena, Colombia, 2018, pp. 830-833, doi: 10.1109/APWC.2018.8503774.
2. Sundaravel M E and P. H. Rao, "Compact printed trapezoidal Koch fractal wide-slot antenna," 2015 IEEE Applied Electromagnetics Conference (AEMC), Guwahati, India, 2015, pp. 1-2, doi:10.1109/AEMC.2015.7509184.
3. Z. Yu, J. Yu, C. Zhu and Z. Yang, "An improved Koch snowflake fractal broadband antenna for wireless applications," 2017 IEEE 5th International Symposium on Electromagnetic Compatibility (EMC-Beijing), Beijing, China, 2017, pp. 1-5, doi: 10.1109/EMC-B.2017.8260462.
4. K. Kavitha, J. Ananthi and M. Parvathi, "Miniaturised Circularly Polarised Koch Fractal Antenna with Rotated Fractal Slot for RFID Applications," 2018 Second International Conference on Electronics, Communication and Aerospace Technology (ICECA), Coimbatore, India, 2018, pp. 1219-1222, doi:10.1109/ICECA.2018.8474590.
5. Y. Zhang, W. Cao, Z. Qian and W. Peng, "An Electrically Large Microstrip Antenna Fed by SICL," 2019 International Conference on Microwave and Millimeter Wave Technology (ICMMT), Guangzhou, China, 2019, pp. 1-3, doi: 10.1109/ICMMT45702.2019.8992418.
6. G. -R. Su, E. S. Li, T. -W. Kuo, H. Jin, Y. -C. Chiang and K. -S. Chin, "79-GHz Wide-Beam Microstrip Patch Antenna and Antenna Array for Millimeter-Wave Applications," in IEEE Access, vol. 8, pp.200823-200833, 2020, doi: 10.1109/ACCESS.2020.3035750.
7. Z. Yan and Y. Xu, "Design and measurement of a differential fed tapered slot UWB antenna," 2016 CIE International Conference on Radar (RADAR), Guangzhou, China, 2016, pp. 1-3, doi:10.1109/RADAR.2016.8059424.
8. J. Wu, Y. Qi, W. Yu, L. Liu and F. Li, "An Absorber-Integrated Taper Slot Antenna," in IEEE Transactions on Electromagnetic Compatibility, vol. 59, no. 6, pp. 1741-1747, Dec. 2017, doi:10.1109/TEM.2017.2714580.
9. H. Kähkönen, J. Ala-Laurinaho and V. Viikari, "Surface-Mounted Ka-Band Vivaldi Antenna Array," in IEEE Open Journal of Antennas and Propagation, vol. 2, pp. 126-137, 2021, doi:10.1109/OJAP.2020.3046465.
10. A. Balanis, Antenna Theory-Analysis and Design, 3rd edition. Hoboken, NJ, USA: Wiley, 2005.